Vibration and Flutter Analysis of Reusable Surface Insulation Panels

EARL H. DOWELL*
Princeton University, Princeton, N.J.

Nomenclature†

a, b = length, width of tile
$a_{i_x i_y}, b_{k_x k_y}$ = generalized coordinates
D = $Et^3/12(1-\nu^2)$, plate stiffness
d = distance between tiles
E = modulus of elasticity
f = frequency, cps
K = $(m_T \omega^2 a^4/D_T)^{1/2}$, nondimensional frequency
K_I = $(E_I t_I/d)/6(1+\nu_I)$
K_{i_x,i_y,j_x,j_y} = stiffness coefficients
k_I = $E_I/t_I(1-\nu_I^2)$
M = Mach number
m = ρt; mass/area
NX, NY = number of tiles in x and y directions, respectively
N_x, N_y, N_{xy} = in-plane stress resultant loadings
p = pressure
q = $\rho_f U^2/2$; dynamic pressure
T = kinetic energy
t = thickness
U = potential elastic energy; also airflow velocity
W = work
w = vertical deflection
x = streamwise coordinate; measured from leading edge of tile
y = spanwise coordinate; measured from side edge of tile
β = $(M^2-1)^{1/2}$
δ = virtual operator
δ_{ij} = Kronecker delta
λ = $2qa^3/MD_T$; nondimensional dynamic pressure M may be replaced by $\beta = (M^2-1)^{1/2}$
μ = $\equiv \rho_f a/\rho_T t_T$; mass ratio
ν = Poisson's ratio
ω = frequency, rad/sec
ρ = density
ζ = damping ratio

Subscripts
F = flutter
f = fluid
I = strain isolator
M = metallic main substructure plate
T = ceramic tile
i_x, i_y, j_x, j_y = modal indices
k_x, k_y, l_x, l_y
n_x, n_y = tile indices

Superscripts
I, M, T = occasionally used as superscripts as needed
Na = a is replaced by N times a

Received June 3, 1974; revision received July 30, 1974. The author would like to thank H. L. Bohon for several helpful suggestions and questions. This work was supported by NASA Grant NGR 31-001-146, Langley Research Center.

Index categories: Aeroelasticity and Hydroelasticity; Structural Dynamic Analysis.

* Professor, Department of Aerospace and Mechanical Sciences. Member AIAA.

† In Pt. I[2] somewhat different notation was used to correspond to that previously employed in the literature. In the present paper more mnemonic notation is introduced.

I. Introduction

A CURRENT design concept for the Thermal Protection System (TPS) heat shield panels of the space shuttle (and other high performance vehicles) consists of a relatively thick ceramic tile mounted on a soft (viscoelastic) foundation, a so-called "strain-isolator," which in turn is bonded to the primary load carrying metal structure.[1] These are generically referred to as Reusable Surface Insulation (RSI) panels. The strain isolator is intended to protect the tile from loads transmitted from the primary structure. While this TPS panel concept has several potential advantages, it represents a substantially unknown quantity from the standpoint of its dynamic stability and response characteristics in the presence of an airflow over its upper surface. Hence, we have undertaken and are reporting here a study of the aeroelastic behavior of such panels. While we shall focus principally on the stability or "flutter" behavior, much of the work is directly relevant to the ("acoustic") response problem.

A simplified sketch of a TPS panel design is given in Fig. 1. Typical characteristics of the geometry and materials are as follows: Ceramic Tile Plate: $E_T = 50{,}000$ psi; $\rho_T = 15$ lb/ft^3; surface dimensions 1 ft × 1 ft; thickness, $t_T = 1$ in.–2 in. Strain Isolator: $E_I = 20$ psi; $\rho_I = 20$ lb/ft^3; and surface dimensions—covers several individual tiles thickness, $t_I = \frac{1}{4}$ in.–$\frac{3}{4}$ in.

It is tempting to model this structure as an elastic panel, the tile, on a uniform elastic foundation, the strain isolator, which in turn is mounted on an essentially rigid base, the primary load carrying metal structure. If one does this the first natural vibration motion is simply that of a uniform (rigid body) translation of the panel on its elastic foundation. Indeed the second (pitching) mode also has a rigid body character and one is further tempted to treat the tile as a rigid body.

If one now proceeds to assess the flutter dynamic pressure, i.e., that dynamic pressure at which the system becomes aeroelastically dynamically unstable, some difficulty arises. Normally one would begin by combining the above structural model with an appropriate aerodynamic flow model. Quasi-steady or

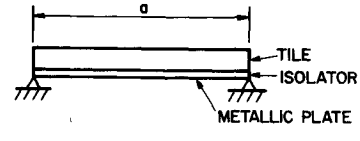

SINGLE TILE

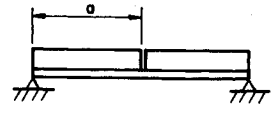

TWO TILES

Fig. 1 TPS RSI panel geometry.

"piston" theory is a particular favorite with analysts as it is simple and reasonably accurate for high supersonic Mach numbers. Frequently a further simplification is made to what has been called the quasi-static model wherein the aerodynamic loading is assumed proportional to the local structural slope and all unsteady or even quasi-steady effects such as aerodynamic damping are ignored. If one employs this simplest aerodynamic model with a rigid plate model of the tile, however, one finds the predicted flutter dynamic pressure is infinite. On the other hand if one uses an elastic plate tile model with the same aerodynamic model, one determines the flutter dynamic pressure is zero. Hence, this paper is devoted to finding a rational aeroelastic model which will provide a finite and reasonably accurate value for the flutter dynamic pressure suitable for use by the designer.

In the process various refinements to the simplified model described previously are considered. These include: 1) effect of aerodynamic damping; 2) multitile effects, i.e., interaction between adjacent tiles; and 3) effect of flexibility of primary load carrying, metallic plate substructure on which the strain isolator rests.

We also discuss some typical numerical examples and provide an assessment of the potential for panel flutter of RSI type panels.

II. Structural and Aerodynamic Modeling

Structural Model

The ceramic tile and metallic plate are each modeled by classical thin plate theory. For reference, numerical results will also be given for the case where the metallic plate is considered rigid. As discussed below the modeling of the isolator is conceptually more subtle.

For a thorough discussion of the structural modeling of the strain isolator see Pt. I.[2] Qualitatively the important distinction is between the Winkler foundation model and what we call the shear foundation model.[2] In the former a point load on the foundation gives rise to a deflection at the same point but nowhere else. Hence the force of the foundation on the ceramic tile at a point is proportional to the tile deflection (which is equal to the surface foundation deflection assuming a perfect tile-foundation bond) at the same point. In the shear foundation model, a point load gives rise not only to a deflection at that point but to surrounding points as well with an exponential decay of deflection away from the point of application of the force. The characteristic length associated with this decay is on the order of the foundation (isolator) thickness. Hence the force of the foundation on the ceramic tile at a point is no longer simply proportional to the deflection at the same point. If two tiles are placed less than a distance of one foundation thickness apart, the shear foundation model is required to describe their interaction. This will frequently be the case. Of course, if a tile length is of the order of a foundation thickness or less (rather unlikely for present applications) the shear foundation model would be required to treat even a single panel. Finally, if a panel (tile) is placed on a foundation (isolator) of infinite extent (i.e., one of sufficient extent that reflected waves from the far boundaries are unimportant) the shear foundation model provides a mechanism for radiation damping which is not possible with the simpler Winkler model. For present RSI configurations only the multitile interaction may require the more complicated foundation model.

Aerodynamic Forces

In determining the aerodynamic forces we normally include both the prescribed external forces such as those due to acoustic sources as well as the aerodynamic forces due to the panel motion itself. Only the latter are important from the standpoint of flutter per se and in the usual acoustic response analysis only the former are included. It has been pointed out, however, that from the standpoint of determining total response both must sometimes be included.[3] Here we shall neglect the external acoustic excitation forces (though they are readily incorporated into the analysis). We shall concentrate instead on the motion dependent aerodynamic forces and their effect on panel flutter. Any of the available levels of aerodynamic theory may be incorporated into the present analysis.[4] For the present we shall use the simplest theory, the so-called "piston" or two-dimensional, quasi-steady theory.

III. Analysis

The basic approach uses a Rayleigh-Ritz technique. For simplicity of exposition we first consider a single, isotropic (spanwise rigid) tile and an isotropic main substructure. The relevant energies and virtual work are as follows:

Elastic Energy

Main Metallic Substructure

$$U = \frac{D^M}{2}\int_0^a\int_0^b\left[\left(\frac{\partial^2 w^M}{\partial x^2}\right)^2+\left(\frac{\partial^2 w^M}{\partial y^2}\right)^2+2\nu^M\frac{\partial^2 w^M}{\partial x^2}\frac{\partial^2 w^M}{\partial y^2}+2(1-\nu^M)\left(\frac{\partial^2 w^M}{\partial x\,\partial y}\right)^2\right]dx\,dy$$
$$+\frac{N_x^M}{2}\int_0^a\int_0^b\left(\frac{\partial w^M}{\partial x}\right)^2 dx\,dy+\frac{N_y^M}{2}\int_0^a\int_0^b\left(\frac{\partial w^M}{\partial y}\right)^2 dx\,dy$$

Tile

$$+\frac{D^T}{2}\int_0^a\int_0^b\left(\frac{\partial^2 w^T}{\partial x^2}\right)^2 dx\,dy$$

Isolator

$$+\frac{k_I}{2}\int_0^a\int_0^b (w^T-w^M)^2\,dx\,dy \tag{1}$$

Kinetic Energy

$$T=\frac{m_T}{2}\int_0^a\int_0^b(\dot{w}^T)^2\,dx\,dy+\frac{m_M}{2}\int_0^a\int_0^b(\dot{w}^M)^2\,dx\,dy \tag{2}$$

Virtual Work due to Aerodynamic Pressure

$$\delta W=-\int_0^a\int_0^b p\,\delta w^T\,dx\,dy \tag{3}$$

where

$$p=\frac{2q}{M}\left[\frac{\partial w^T}{\partial x}+\frac{1}{U}\frac{\partial w^T}{\partial t}\right] \tag{4}$$

and

$$k_I = E_I/t_I(1-\nu_I^2)$$

Note we have included in-plane loads N_x and N_y. Let

$$w^T=\sum_{i_x}\sum_{i_y}a_{i_xi_y}(t)\phi_{i_x}(x)\phi_{i_y}(y)$$
$$w^M=\sum_{k_x}\sum_{k_y}b_{k_xk_y}(t)\psi_{k_x}(x)\psi_{k_y}(y) \tag{5}$$

where $\psi_{k_x}\psi_{k_y}$ are the natural modes of a simply-supported plate and ϕ_{i_x}, ϕ_{i_y} those of a free-free beam. Then

$$U=\frac{D^M}{2}\sum_{k_x}\sum_{k_y}b_{k_xk_y}^2\left[\left(\frac{k_y\pi}{a}\right)^2+\left(\frac{k_y\pi}{b}\right)^2\right]^2\frac{a}{2}\frac{b}{2}+$$
$$\frac{N_x^M}{2}\sum_{k_x}\sum_{k_y}b_{k_xk_y}^2\left(\frac{k_x\pi}{a}\right)^2\frac{ab}{4}+\frac{N_y}{2}\sum_{k_x}\sum_{k_y}b_{k_xk_y}^2\left(\frac{k_y\pi}{b}\right)^2\frac{ab}{4}+$$
$$\frac{D^T}{2}\sum_{i_x}\sum_{i_y}a_{i_xi_y}^2\int_0^a\left(\frac{d^2}{dx^2}\phi_{ix}\right)^2dx\int_0^b\phi_{i_y}^2\,dy+$$
$$\frac{k_I}{2}\left\{\sum_{i_x}\sum_{i_y}a_{i_xi_y}^2ab+\sum_{k_x}\sum_{k_y}b_{k_xk_y}^2\frac{ab}{4}-\right.$$
$$\left.2\sum_{i_x}\sum_{i_y}\sum_{k_x}\sum_{k_y}a_{i_xi_y}b_{k_xk_y}\int_0^a\phi_{i_x}\psi_{k_x}dx\int_0^b\phi_{i_y}\psi_{k_y}dy\right\} \tag{6}$$

$$T=\frac{m_T}{2}\sum_{i_x}\sum_{i_y}\dot{a}_{i_xi_y}^2ab+\frac{m_M}{2}\sum_{k_x}\sum_{k_y}\dot{b}_{k_xk_y}^2\frac{ab}{4} \tag{7}$$

Note

$$\int\int \phi_{i_x}(x)\phi_{i_y}(y)\,\phi_{j_x}(x)\phi_{j_y}(y)\,dx\,dy = \delta_{i_x j_x}\,\delta_{i_y j_y}\,ab$$

$$\int\int \psi_{k_x}(x)\psi_{k_y}(y)\psi_{l_x}(x)\psi_{l_y}(y)\,dx\,dy = \delta_{k_x l_x}\,\delta_{k_y l_y}\,\frac{ab}{4}$$

$$\int_0^a \left(\frac{d^2}{dx^2}\phi_{i_x}\right)^2 dx = \frac{\beta_i{}^4}{a^4}$$

and

$$\delta W = \sum_{i_x}\sum_{i_y} Q_{i_x i_y}\,\delta a_{i_x i_y} \tag{8}$$

where

$$Q_{i_x i_y} = \frac{2q}{M}\left\{\sum_{j_x}\sum_{j_y} a_{j_x j_y}\int_0^a\int_0^a \frac{d\phi_{j_x}}{dx}\phi_{i_x}\phi_{j_y}\phi_{i_y}\,dx\,dy + \frac{\dot{a}_{j_x j_y}}{U}\int_0^a\int_0^a \phi_{j_x}\phi_{i_x}\phi_{j_y}\phi_{i_y}\,dx\,dy\right\} \tag{9}$$

Using Lagrange's equations, we obtain

$$m_M\,\ddot{b}_{k_x k_y} + b_{k_x k_y}\left\{D_M\left[\left(\frac{k_x\pi}{a}\right)^2+\left(\frac{k_y\pi}{b}\right)^2\right]^2 + N_x\left(\frac{k_x\pi}{a}\right)^2 + N_y\left(\frac{k_y\pi}{b}\right)^2\right\} + k_I\,b_{k_x k_y} - 4k_I\sum_{i_x}\sum_{i_y} a_{i_x i_y}\int_0^a\int_0^b \phi_{i_x}\phi_{i_y}\psi_{k_x}\psi_{k_y}\frac{dx}{a}\frac{dy}{b} = 0 \qquad k_x, k_y = 1,\ldots \tag{10}$$

and

$$m_T\,\ddot{a}_{i_x i_y} + D_T\frac{\beta_i{}^4}{a^4}a_{i_x i_y} + k_I\,a_{i_x i_y} - k_I\sum_{k_x}\sum_{k_y} b_{k_x k_y}\int_0^a\int_0^b \phi_{i_x}\phi_{i_y}\psi_{k_x}\psi_{k_y}\frac{dx}{a}\frac{dy}{b} = \frac{Q_{i_x i_y}}{ab} \qquad i_x, i_y = 1,\ldots \tag{11}$$

At times by an examination of the mass, stiffness, and natural modes of the system for typical parameter values one can, without loss of essential accuracy, neglect the inertia of the metallic plate, i.e., set $m_M \equiv 0$. This substantially simplifies the calculation in that one may then solve for $b_{k_x k_y}$ in terms of $a_{i_x i_y}$ from Eq. (10). Substitution into Eq. (11) gives

$$m_T\,\ddot{a}_{i_x i_y} + a_{i_x i_y}\frac{D_T}{a^4}\left[\beta_i{}^4 + \frac{k_I}{D}a^4\right] + \sum_{j_x}\sum_{j_y} K_{i_x i_y j_x j_y}\,a_{j_x j_y} = \frac{Q_{i_x i_y}}{ab} \tag{12}$$

where

$$K_{i_x i_y j_x j_y} \equiv -4k_I{}^2\sum_{k_x}\sum_{k_y}\left[\int_0^a\int_0^b \phi_{j_x}\phi_{j_y}\psi_{k_x}\psi_{k_y}\frac{dx}{a}\frac{dy}{b}\right]\times\left[\int_0^a\int_0^b \phi_{i_x}\phi_{i_y}\psi_{k_x}\psi_{k_y}\frac{dx}{a}\frac{dy}{b}\right] \Big/ \left\{D_M\left[\left(\frac{k_x\pi}{a}\right)^2+\left(\frac{k_y\pi}{b}\right)^2\right]^2 + N_x\left(\frac{k_x\pi}{a}\right)^2 + N_y\left(\frac{k_y\pi}{b}\right)^2 + k_I\right\}$$

One may now study the stability of the system by determining whether solutions for the $a_{i_x i_y}$ and $b_{k_x k_y}$ decay or grow with time, either using Eqs. (10) and (11) or the simpler Eq. (12) as appropriate.

It should be emphasized that the neglect of the metallic plate inertia appears reasonable for preliminary design analyses of RSI panels; however, more refined studies may need to include this inertia. Moreover this approximation will be more reliable for flutter analysis than for acoustic response or even natural mode and frequency analysis. This is because the flutter behavior of panels is usually rather insensitive to structural mass and primarily determined by structural stiffness.

The generalization of the abovementioned analysis to any number of orthotropic tiles with spanwise flexibility and orthotropic metallic substructures, is discussed in Appendix A.

IV. Representative Flutter Results

Before considering the full structural model, we first study for reference purposes the special case of a rigid metallic substructure, $D^M \to \infty$. As we shall see, however, this is not a reasonable model for typical space shuttle designs.

A. Rigid Metallic Substructure—Single Tile

Using the simplest isolator model wherein the isolator forces are proportional to plate displacement (Winkler model), we find that for a rigid plate tile no flutter can occur. The situation is similar to that of a rigid airfoil where the center of mass and elastic axes coincide. Conversely if the tile is elastic but no (aerodynamic or structural) damping is included in the analysis the tile will always flutter for any dynamic pressure. This is because, without damping, the Winkler elastic foundation has no effect on flutter dynamic pressure[5] and hence the flutter behavior is the same as that of an unsupported plate tile. With damping included, flutter occurs above some finite dynamic pressure but not below it. Such results are shown in Fig. 2 with aerodynamic damping, but no structural damping, included. Flutter dynamic pressure is plotted vs foundation stiffness for various air/panel mass ratios, μ/M. The strength of the aerodynamic damping is proportional to $(\lambda\mu/M)^{1/2}$. An equivalent *structural* damping ratio is

$$\zeta_{\text{ref}} = (\lambda\mu/M)^{1/2}/2K_{\text{ref}}$$

where ζ_{ref} is a critical damping ratio based upon a (nondimensional) reference frequency K_{ref}. Hence the results may be interpreted in terms of viscous, structural as well as aerodynamic damping.

Using the more refined shear foundation model (Pt. I) which allows for extended foundation reaction, we have computed flutter dynamic pressure for a few representative single tile cases. These results are not essentially different from those obtained using the Winkler model.

To consider a concrete numerical example, we take $\rho_T = 15\#/\text{ft}^3$; $E_T = 50\times10^3$ psi; $\rho_I = 20\#/\text{ft}^3$; $E_I = 20$ psi; $t_T = 0.5$ in.; $t_I = 1$ in.; $\nu_I = \nu_T = 0.3$; $a = 20$ in.; and $a/b = 0$.

We also choose $M = 2$, $\mu/M = 0.1$, corresponding to sea level conditions. We determine the (nondimensional) flutter dynamic pressure and frequency as $\lambda_F = 680$, $K_F = 63$, and the dimensional flutter dynamic pressure is $q_F = 42$ psi. Hence one concludes flutter is unlikely, given such large q_F, even allowing for moderate parameter variations.

Multiple tiles

A more realistic panel model is one which accounts for the interaction between adjacent plate tiles. Here the Winkler

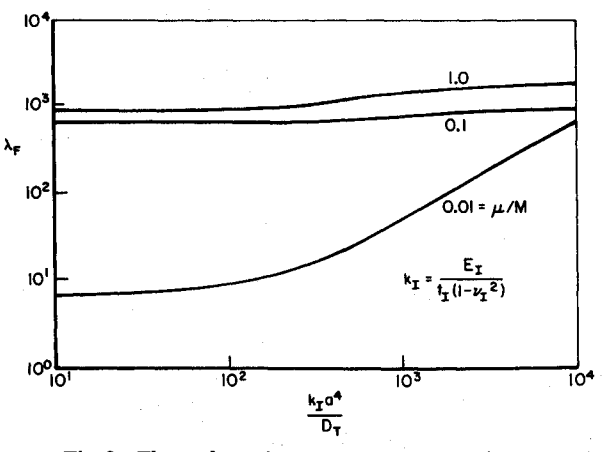

Fig. 2 Flutter dynamic pressure vs isolator stiffness.

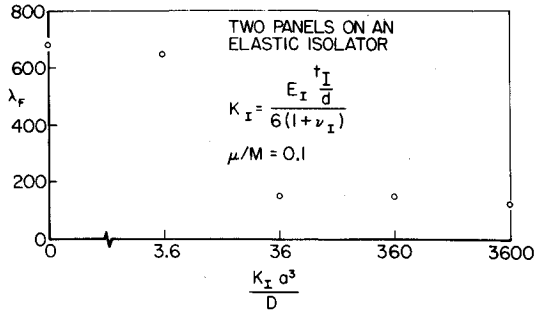

Fig. 3 Flutter dynamic pressure vs connecting spring stiffness.

foundation model is wholly inadequate (for a rigid metallic substructure) since it does not allow any interaction between adjacent plates. Instead the shear foundation model must be used. Since, however, closely spaced panels are of primary interest we may use a simplified equivalent spring model to account for inter-tile interaction. In this model two adjacent tiles are assumed to be connected by a vertical spring at their edges. See Sec. 5, Pt. I, where the equivalent spring is determined to be (also see Appendix A)

$$K_I = (E_I t_I/d)/6(1+\nu_I)$$

As an example, a two-tile configuration using the dimensions previously chosen for a single panel has been studied. The distance between panels is initially taken as $d = 0.1$ in.

It is found that $\lambda_F = 150$, $K_F = 60$, and $q_F = 9.4$ psi where $K_I a^3/D_T = 360$. Other $d(K_I \sim 1/d)$ were also considered and the results are shown in Fig. 3. For $K_I a^3/D \to \infty$, $\lambda_F \to 0$ while for $K_I a^3 D \to 0$, λ_F approaches the single panel result. An analytical solution for the *rigid* tile model with two tiles connected by an elastic spring has been obtained to help interpret the former limit.

The principal conclusion drawn from the above is that multitile interaction may be important and harmful, i.e., it leads to lower flutter dynamic pressures than for a single panel. Fortunately, a simple cut in the isolator between tiles will remove this effect. Such a cut is part of the present space shuttle design.

B. Flexible Metallic Substructure

The previous results are for an elastic (relatively stiff) plate, the "tile," resting on a continuous elastic (soft) foundation, the "isolator," which in turn is on a rigid base. In the proposed space shuttle design, this "rigid base" is in reality an elastic plate resting between supports (see Fig. 1). Hence we need to include in our model the flexibility of this foundation plate. For typical parameter values, the flexibility of the foundation decreases the over-all system stiffness and corresponding flutter dynamic pressure by a factor of ten or more. Hence it dominates the TPS dynamics.

A representative set of calculations has been completed which illustrates the importance of the various parts of the structural model and the sensitivity of the flutter dynamic pressure parameter q_F/M to various model parameters. We note that from our analysis we may also determine natural modes as well as flutter boundaries (see Appendix B). Initially the following parameters were used (see Table 1).

Table 1 Nominal case, sea level air density

Tile	$E_T = 50 \times 10^3$ psi $t_T = 1$ in.	$\rho_T = 15\#/\text{ft}^3$
Isolator	$E_I = 20$ psi $t_I = \frac{1}{4}$ in.	
Foundation	$E_M = 10^7$ psi $t_M = 0.020$ in.	$\rho_M = 0.1\#/\text{in}^3$

Table 2 One tile results

	$t_I = 0.25''$	
	$a = 10$ in.	20 in.
$t_T = 1$ in.	$q_F/M = 20$ psi $f_F = 126$ cps	12.5 psi 87 cps
0.5 in.	12.5 psi 172 cps	7.5 psi 134 cps
	$a = 20$ in.	
	$t_I = 0.25$	0.5 in.
$t_T = 1$ in.	12.5 psi 87 cps	10 psi 66 cps
0.5 in.	7.5 psi 134 cps	6 psi 65 cps

The length of the foundation and isolator is 20 in. and that of the tile a varies (depending on the number of tiles per foundation plate). The length/width ratio is zero. The foundation plate is assumed simply supported and the tile rests freely on the isolator. It will be of interest to first record, for reference, results from certain idealized, structural models.

For the metallic plate alone (of length 20 in.)

$$q_F/M = 0.15 \text{ psi} \qquad f_F = 14 \text{ cps}$$

For the tile alone (assuming it is simply supported, which it is not, and of length 10 in.)

$$q_F/M = 700 \text{ psi} \qquad f_F = 690 \text{ cps}$$

In both of the abovementioned aerodynamic damping has been ignored. *The point of the above is to demonstrate that the softness of the foundation may be expected to have an important effect on over-all system behavior.* One further idealized reference case (see Sec. a) is that of the elastic tile freely resting on the isolator with a rigid metallic plate. Without (aerodynamic) damping $q_F = 0$! With aerodynamic damping 'for sea level conditions) $q_F/M = 800$ psi! With aerodynamic damping (for 30,000 ft altitude) $q_F/M = 20$ psi. Hence this idealized model is very sensitive to the amount of damping in the system.

Now let us turn to the full model, a tile resting freely on the isolator which is attached to a flexible, simply supported metallic plate. First consider only a single tile; these results are summarized in Table 2 for several parameter variations about the nominal case. Sea level density is assumed; a high altitude (lower density) would reduce q_F/M by a modest amount but not nearly as much for the case where the foundation is assumed rigid. *The significant conclusion is that the effect of the flexible foundation is very important in reducing flutter dynamic pressure.*

The effects of length to width ratio have been examined for the nominal single tile and the results are shown in Fig. 4.

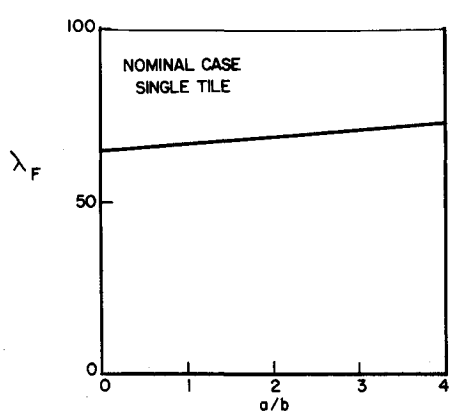

Fig. 4 Effect of length width ratio on flutter.

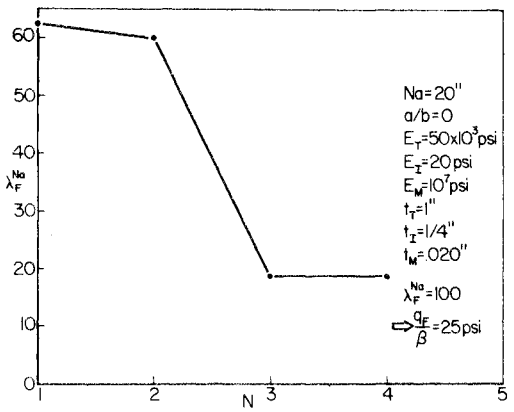

Fig. 5 Flutter dynamic pressure vs tile number, nominal case.

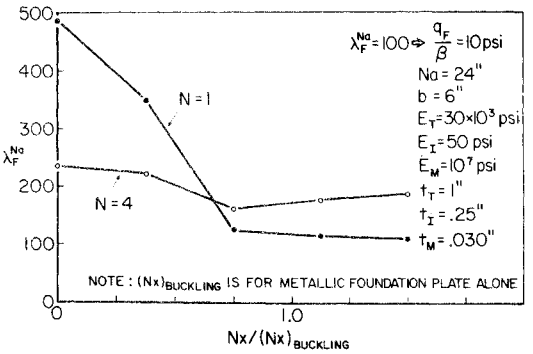

Fig. 7 Flutter dynamic pressure vs in-plane load.

Unlike more conventional plates[5] there is *very little increase* in flutter dynamic pressure due to length/width ratio. Presumably this is associated with the relative rigidity of the tile.

The effect of multiple tiles has also been studied. In Fig. 5 results are shown for up to four tiles. Here the total aluminum panel length Na is held constant, while the tile number N and length a are varied. Na is used as a normalizing length for this comparison. As expected the flutter dynamic pressure decreases with increasing N. The isolator is assumed cut between tiles. Note that for all parameter variations studied, the flutter dynamics pressure is well above that for the metallic foundation plate alone.

As a final example we have considered a configuration representative of an early cargo bay door design of the Space Shuttle. Here we focus on the effects of compressive preload, tile number and tile thickness.

Space Shuttle Example

For our calculations we have taken a simply-supported, aluminum substructure plate with $Na = 24$ in., length; $b = 6$ in., width; $E_M = 10^7$ psi, elastic modulus; and $t_M = 0.1\,\#/\text{in}^3$, density. On top of this plate there is a strain isolator with $Na = 24$ in., $b = 6$ in., $E_I = 50$ psi, $t_I = 0.25$ in., $\rho_I = 20\ \#/\text{ft}^3$. On top of this isolator there are ceramic tiles with $a = 24$ in., 12 in., 8 in., 6 in. ($N = 1, 2, 3, 4$), $b = 6$ in., $E_T = 30 \times 10^3$ psi, $t_T = 1$ in., $\rho_T = 9\ \#/\text{ft}^3$, and N = number of tiles. Piston theory aerodynamics are employed and sea level conditions are assumed.

In Fig. 6 (nondimensional) flutter dynamic pressure is plotted vs number of tiles. There is a measurable but not overwhelming effect of tile number on flutter dynamic pressure. It should be mentioned, however, that as before the isolator between tiles has been assumed cut so that there is no effective spring connection between tiles due to their lying on a common isolator. The effect of such a spring connection would be to further decrease the flutter dynamic pressure.

In Fig. 7, the effect of an in-plane, compressure, normal load on flutter dynamic pressure is shown for one and four tiles. Note that the normalizing factor for N_x is the buckling load for the metallic foundation plate alone. The buckling load for the total structure including isolator and tile is higher and indeed, for the range of in-plane loads shown, no buckling occurs. Nevertheless there is a substantial reduction in flutter dynamic pressure for one tile but not four. Single tile results were also obtained (not shown) for compressive shear loads up to twice the buckling load for the aluminum plate alone. Virtually no change in flutter dynamic pressure was observed. Current design practice is to avoid buckling on the space shuttle.

As an alternative to the above model, an orthotropic main plate was considered with infinite width, $a/b = 0$, and an appropriate average stiffness based upon the combined plate and stringer support stiffnesses. The flutter dynamic pressure was much higher. As another reference value, the (dimensional) flutter dynamic pressure for the metallic foundation plate alone (isotropic with $a/b = 4$) is approximately (neglecting aerodynamic damping)

$$q_F/\beta = 4 \text{ psi}$$

Hence the addition of the isolator and tiles is again stabilizing with respect to flutter (and also as noted above with respect to buckling).

As a final parameter variation we have considered the effect of tile thickness on flutter dynamic pressure. Perhaps surprisingly,

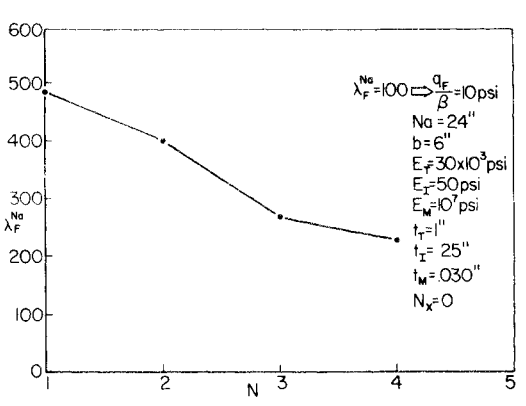

Fig. 6 Flutter dynamic pressure vs tile number, cargo bay door.

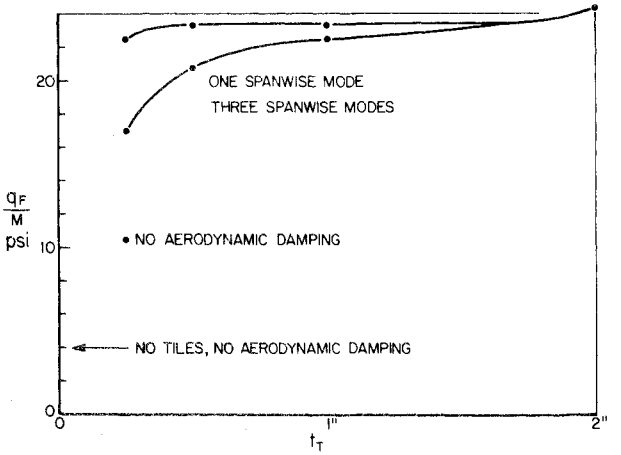

Fig. 8 Flutter dynamic pressure vs tile thickness.

there is very little sensitivity to tile thickness for the range of anticipated design values (see Fig. 8). As a matter of interest we have shown results for one spanwise tile mode (rigid body translation) and three spanwise tile modes (rigid body translation, rigid body rotation, first symmetric elastic bending). As can be seen, these begin to differ for $t_T < 0.5$ in. For large t_T the tile is essentially rigid spanwise and flutters in a symmetric mode. For smaller t_T the flutter mode remains symmetric but the tile now elastically deforms and follows the half-sine wave of the metallic plate foundation. For reference, we also show in Fig. 8 the flutter dynamic pressure for $t_T = 0.25$ in. and no aerodynamic damping and that for the metallic foundation plate alone with no aerodynamic damping. Note that as $t_T \to 0$ the results do appear to approach those of the metallic foundation plate alone.

In summary for the range of parameters studied (assigning $\beta = 1$ as a rough value), flutter dynamic pressure, 10–20 psi, is above the anticipated maximum flight trajectory dynamic pressure value of 5 psi. However, more refined aerodynamic models for low supersonic Mach numbers could modify these results.

Further Studies

Further work needs to be done. The forced vibration problem where, for example, the plate responds to boundary-layer noise should be examined in the context of the present models.

Moreover improvements in the present models may be needed for certain applications. The isolator is viscoelastic in nature rather than elastic; hence the material damping in the isolator is apt to be important and, indeed, may dominate over the aerodynamic and foundation radiation damping mechanisms considered here. Measurements need to be made on representative materials to characterize the viscoelasticity of the isolator. Also the material nonlinearity may be important as well.

At the lower Mach numbers, aerodynamic induction may be important and one might anticipate some spanwise interaction between adjacent panels. In any event, a more accurate (and unfortunately more complicated) aerodynamic theory is required to study the problem at low supersonic Mach numbers. Also, if the strain isolator is cut between tiles, there will be deflection discontinuities from tile to tile whose effect on the aerodynamic forces remains to be evaluated (see Appendix B).

Conclusions

An analytical aeroelastic model of a Reusable Surface Insulation panel system has been developed from which natural modes and flutter stability boundaries may be determined. For parameters representative of Space Shuttle, the metallic foundation plate dominates the flexibility of the system and, hence, its flutter behavior. The addition of tiles and isolator stiffens the system and their effect, in the examples studied, was to raise the flutter dynamic pressure over that of the metallic foundation plate alone. Also, inter alia it was determined that there is a substantial increase in the (inter-stringer) buckling load due to the addition of isolator and tiles.

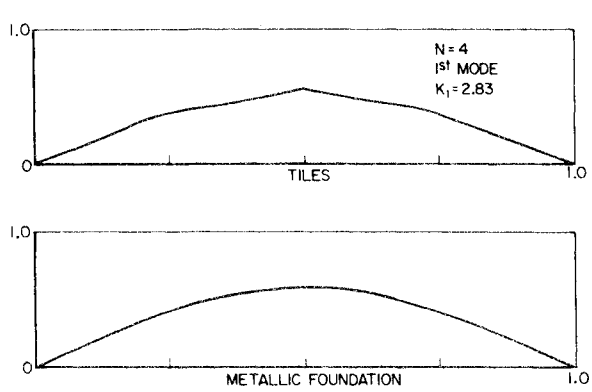

Fig. 9 Center line deflection, 1st mode.

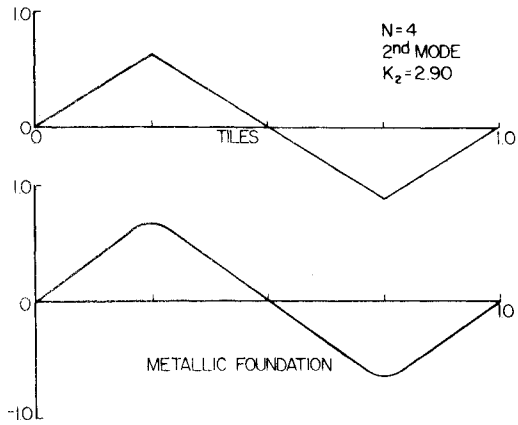

Fig. 10 Center line deflection, 2nd mode.

Appendix A: Multitile Formulation

Elastic Energy

Main Metallic Substructure

$$U = \frac{1}{2}\int_0^{NXa}\int_0^{NYb}\left[D_x{}^M\left(\frac{\partial^2 w^M}{\partial x^2}\right)^2 + D_y{}^M\left(\frac{\partial^2 w^M}{\partial y^2}\right)^2 + 2D_1{}^M\frac{\partial^2 w^M}{\partial x^2}\frac{\partial^2 w^M}{\partial y^2} + 4D_{xy}{}^M\left(\frac{\partial^2 w^M}{\partial x\,\partial y}\right)^2\right]dx\,dy + \frac{1}{2}\int_0^{NXa}\int_0^{NYb}\left[N_x{}^M\left(\frac{\partial w^M}{\partial x}\right)^2 + N_y{}^M\left(\frac{\partial w^M}{\partial y}\right)^2 + 2N_{xy}{}^M\frac{\partial w^M}{\partial x}\frac{\partial w^M}{\partial y}\right]dx\,dy +$$

Tile

$$\frac{1}{2}\sum_{n_x=1}^{NX}\sum_{n_y=1}^{NY}\int_{(n_x-1)a}^{n_x a}\int_{(n_y-1)b}^{n_y b}\left\{D_x{}^T\left(\frac{\partial^2 w^T_{n_x n_y}}{\partial x^2}\right)^2 + D_y{}^T\left(\frac{\partial^2 w^T_{n_x n_y}}{\partial y^2}\right)^2 + 2D_1{}^T\frac{\partial^2 w^T_{n_x n_y}}{\partial x^2}\frac{\partial^2 w^T_{n_x n_y}}{\partial y^2} + 4D_{xy}{}^T\left(\frac{\partial^2 w^T_{n_x n_y}}{\partial x\,\partial y}\right)^2 +$$

Isolator

$$k_I(w^T_{n_x n_y} - w^M)^2 + K_I[w^T_{(n_x-1)n_y}\delta(x-a) - w^T_{n_x n_y}\delta(x)]^2 + K_I[w^T_{n_x(n_y-1)}\delta(y-b) - w^T_{n_x n_y}\delta(y)]^2\Big\}\,dx\,dy \qquad \text{(A1)}$$

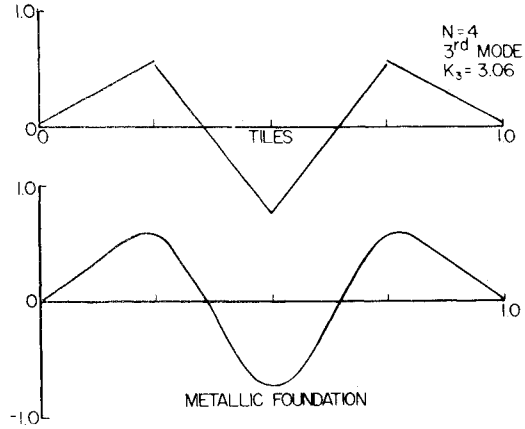

Fig. 11 Center line deflection, 3rd mode.

Kinetic energy

$$T = \frac{m_M}{2}\int_0^{NXa}\int_0^{NYb}(\dot{w}^M)^2\,dx\,dy + \frac{m_T}{2}\sum_{n_x=1}^{NX}\sum_{n_y=1}^{NY}\int_{(n_x-1)a}^{n_x a}\int_{(n_y-1)b}^{n_y b}(\dot{w}^T_{n_x n_y})^2\,dx\,dy \qquad \text{(A2)}$$

where again

$$k_I = \frac{E_I}{t_I(1-\nu_I^2)}$$

$$K_I = \frac{E_I t_I/d}{6(1+\nu_I)} \quad \text{(see Pt. I or Ref. 2)}$$

Virtual Work due to Aerodynamic Pressure

$$\delta W = -\sum_{n_x=1}^{NX}\sum_{n_y=1}^{NY}\int_{(n_x-1)a}^{n_x a}\int_{(n_y-1)b}^{n_y b} P_{n_x n_y}\,\delta w^T_{n_x n_y}\,dx\,dy \qquad \text{(A3)}$$

where

$$P_{n_x n_y} = \frac{2q}{M}\left[\frac{\partial w^T_{n_x n_y}}{\partial x} + \frac{1}{U}\frac{\partial w^T_{n_x n_y}}{\partial t}\right] \qquad \text{(A4)}$$

Proceeding as before, we expand

$$w^T = \sum_i a_{n_x n_y i_x i_y}\phi_{i_x}(x)\phi_{i_y}(y)$$

$$w^M = \sum_{k_x}\sum_{k_y} b_{k_x k_y}\psi_{k_x}(x)\psi_{k_y}(y)$$

to obtain modal equations for $a_{n_x n_y i_x i_y}$ and $b_{k_x k_y}$ via Lagrange's equations. Further details are omitted in the interests of brevity.

Appendix B: Natural Modes

For the space shuttle cargo bay door example with $N = 4$ and $t_T = 1$ in., the natural modes and frequencies have been determined. The first four of these are shown in Figs. 9–12. For the lowest modes the four tiles behave very much as rigid bodies. For reference the flutter frequency is $K_F{}^a = 3.8$. In the flutter and natural mode calculations, 12 chordwise and three spanwise metallic foundation modes were used. Four chordwise and one spanwise modes per tile were employed. Convergence studies were conducted using various modal combinations to assure accuracy of the results.

In general there is a discontinuity in tile deflection from one tile to the next when the strain isolator is cut between tiles. For the modes shown it is most pronounced in the fourth mode (Fig. 12). It is interesting to speculate on what effect this will have on the aerodynamic forces due to tile motion. No available theory would appear adequate and experimental data are needed to assess this effect quantitatively.

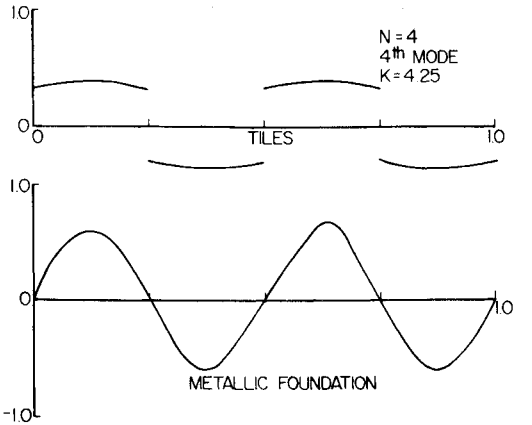

Fig. 12 Center line deflection, 4th mode.

References

[1] Bohon, H. L., "Thermal Protection Systems for Space Shuttle," in D. Greenshields, G. Strouhal, D. Tillian, J. Pawloski, "Development Status of Reusable Non-metallic Thermal Protection," TMX-2273, April 1971, NASA.

[2] Dowell, E. H., "Dynamic Analysis of an Elastic Plate on a Thin, Elastic Foundation," *Journal of Sound and Vibration*, Vol. 35, No. 3, 1974, pp. 343–360.

[3] Dowell, E. H., "Noise or Flutter or Both?," *Journal of Sound and Vibration*, Vol. 11, No. 2, 1970, pp. 159–180.

[4] Dowell, E. H., "Panel Flutter: A Review of the Aeroelastic Stability of Plates and Shells," *AIAA Journal*, Vol. 8, No. 3, March 1970, pp. 385–399.

[5] Dugundji, J., "Theoretical Considerations of Panel Flutter at High Supersonic Mach Numbers," *AIAA Journal*, Vol. 4, No. 7, July 1966, pp. 1257–1266.